Targeted Collaboration on Gas Turbine Combustion: Turbulent Lean Premixed Combustion with Hydrogen Enrichment

Clinton P. T. Groth and Ömer L. Gülder

University of Toronto Institute for Aerospace Studies
4925 Dufferin Street, Toronto, Ontario, M3H 5T6

28th Task Leader's Meeting of IEA Implementing Agreement on Energy Conservation and Emission Reduction in Combustion, Heidelberg, Germany, August 13–16, 2006

Outline

Introduction & Motivation

Canadian Research Initiative

Mathematical Modelling

Computational Framework

Thickened Flame SFS Model

Flame Surface Density SFS Model

G-Equation SFS Model

Concluding Remarks

Outline

Outline

- Introduction & Motivation
- Canadian Research Initiative
- Mathematical Modelling
- Computational Framework
- Thickened Flame SFS Model
- Flame Surface Density SFS Model
- G-Equation SFS Model
- Concluding Remarks

Outline

Outline

Outline

Outline

Outline

Motivation

- Development of capabilities for modelling and prediction of premixed combustion under gas-turbine-like conditions
  - high pressures and temperatures
  - lean hydrocarbon fuels with hydrogen enrichment
- Lean Premixed Combustion with Hydrogen Enrichment
  - high efficiency gas turbine combustion
  - reduced carbon dioxide production and NOx emissions
  - paves the way for hydrogen combustion
- Technical Challenges
  - flame stability, sensitivity to fuel-to-air ratio fluctuations and thermo-acoustic oscillations
  - issues: local extinction, combustion instabilities, blow out, and flash back
  - theoretical and computational models unable to fully explain experimental observations

Motivation

- Development of capabilities for modelling and prediction of premixed combustion under gas-turbine-like conditions
  - high pressures and temperatures
  - lean hydrocarbon fuels with hydrogen enrichment
- Lean Premixed Combustion with Hydrogen Enrichment
  - high efficiency gas turbine combustion
  - reduced carbon dioxide production and NOx emissions
  - paves the way for hydrogen combustion
- Technical Challenges
  - flame stability, sensitivity to fuel-to-air ratio fluctuations and thermo-acoustic oscillations
  - issues: local extinction, combustion instabilities, blow out, and flash back
  - theoretical and computational models unable to fully explain experimental observations

Motivation

- Development of capabilities for modelling and prediction of premixed combustion under gas-turbine-like conditions
  - high pressures and temperatures
  - lean hydrocarbon fuels with hydrogen enrichment
- Lean Premixed Combustion with Hydrogen Enrichment
  - high efficiency gas turbine combustion
  - reduced carbon dioxide production and NOx emissions
  - paves the way for hydrogen combustion
- Technical Challenges
  - flame stability, sensitivity to fuel-to-air ratio fluctuations and thermo-acoustic oscillations
  - issues: local extinction, combustion instabilities, blow out, and flash back
  - theoretical and computational models unable to fully explain experimental observations

Numerical Modelling of Premixed Combustion

Large Eddy Simulations (LES)

- intermediate between DNS and RANS: larger-scale motions resolved
- separation of scales via a low-pass spatial filtering procedure
- proving to be a valuable in modelling turbulent non-reacting flows
- while promising, still under development for turbulent reactive flows

Some of the Challenges

- complex chemical kinetics
- chemical reaction scales smaller than filter size
- in many cases, turbulence-chemistry interactions must be entirely modelled
- control of numerical, filtering (commutation and aliasing), subfilter scale modelling errors

Numerical Modelling of Premixed Combustion

Large Eddy Simulations (LES)

- intermediate between DNS and RANS: larger-scale motions resolved
- separation of scales via a low-pass spatial filtering procedure
- proving to be a valuable in modelling turbulent non-reacting flows
- while promising, still under development for turbulent reactive flows

Some of the Challenges

- complex chemical kinetics
- chemical reaction scales smaller than filter size
- in many cases, turbulence-chemistry interactions must be entirely modelled
- control of numerical, filtering (commutation and aliasing), subfilter scale modelling errors

Borghi-Peters Regime Diagram

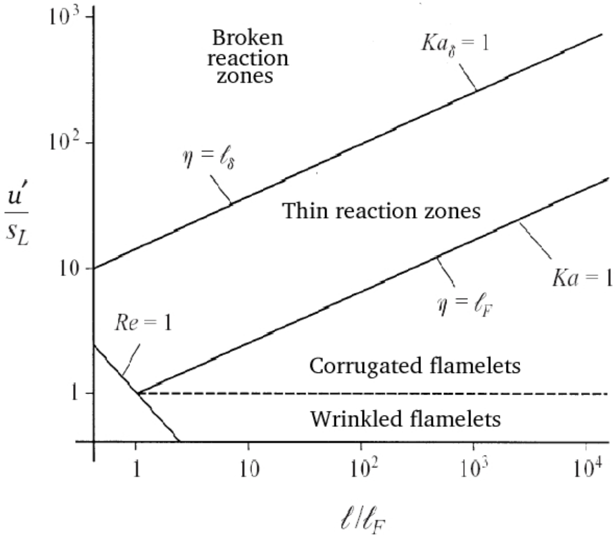

Canadian Research Initiative

Collaborators

- Ö. Gülder and C. Groth (University of Toronto)
- G. Smallwood, F. Liu, H. Guo (NRC ICPET)
- 7-8 graduate students

Research

- Numerical and experimental research program
- 5 numerical tasks
- 3 experimental tasks

A Key Outcome

- development of Large Eddy Simulation (LES) capabilities for turbulent lean premixed combustion

Canadian Research Initiative

Collaborators

- Ö. Gülder and C. Groth (University of Toronto)
- G. Smallwood, F. Liu, H. Guo (NRC ICPET)
- 7-8 graduate students

Research

- Numerical and experimental research program
- 5 numerical tasks
- 3 experimental tasks

A Key Outcome

- development of Large Eddy Simulation (LES) capabilities for turbulent lean premixed combustion

Canadian Research Initiative

Collaborators

- Ö. Gülder and C. Groth (University of Toronto)
- G. Smallwood, F. Liu, H. Guo (NRC ICPET)
- 7-8 graduate students

Research

- Numerical and experimental research program
- 5 numerical tasks
- 3 experimental tasks

A Key Outcome

- development of Large Eddy Simulation (LES) capabilities for turbulent lean premixed combustion

Numerical Tasks

- Subgrid Scale Modelling: Thickened Flame with Power-Law Flame Wrinkling Subgrid Scale Model for Lean-Premixed Combustion
- Subgrid Scale Modelling: Flame Surface Density (FSD) Subgrid Scale Model for Lean-Premixed Combustion
- Subgrid Scale Modelling: G-Equation Subgrid Scale Model for Lean-Premixed Combustion
- LES: Development of Grid-Independent LES Capabilities for Turbulent Reacting Flows
- Hydrogen Enrichment: Effects of Hydrogen/Reformation Gas Addition on Flammability Limit and NOx Emission in Lean Counterflow CH4/Air Premixed Flames

LES Filtering

Low-pass spatial filtering of flow quantities $\mathcal{G}$:

$$\bar{\mathcal{G}}(\mathbf{x},t) = \int\int\int_{V_{sf}} F(\mathbf{x}-\mathbf{x}';\Delta(\mathbf{x}))\mathcal{G}(\mathbf{x}',t)\; d^3\mathbf{x}'$$

Mass-weighted (Favre) spatial filtering:

$$\bar{\rho}\tilde{\mathcal{G}}(\mathbf{x},t) = \int\int\int_{V_{sf}} \rho F(\mathbf{x}-\mathbf{x}';\Delta(\mathbf{x}))\mathcal{G}(\mathbf{x}',t)\; d^3\mathbf{x}'$$

Consistency:

$$\int\int\int_{V_{sf}} F(\mathbf{x}-\mathbf{x}')\; d^3\mathbf{x}' = 1$$

Filtered Navier-Stokes Equations

$$\frac{\partial \bar{\rho}}{\partial t} + \frac{\partial (\bar{\rho}\tilde{u}_j)}{\partial x_j} = 0$$

$$\frac{\partial (\bar{\rho}\tilde{u}_i)}{\partial t} + \frac{\partial (\bar{\rho}\tilde{u}_i\tilde{u}_j + \delta_{ij}\bar{p})}{\partial x_j} - \frac{\partial \tilde{\sigma}_{ij}}{\partial x_j} = -\underbrace{\frac{\partial \tau_{ij}}{\partial x_j}}_{\mathbf{I}} + \underbrace{\frac{\partial (\bar{\sigma}_{ij} - \tilde{\sigma}_{ij})}{\partial x_j}}_{\mathbf{II}}$$

$$\frac{\partial (\bar{\rho}\widetilde{Y}_n)}{\partial t} + \frac{\partial (\bar{\rho}\widetilde{Y}_n\tilde{u}_j)}{\partial x_j} + \frac{\partial \widetilde{J}_{j,n}}{\partial x_j} = -\underbrace{\frac{\partial [\bar{\rho}(\widetilde{Y_n u_j} - \widetilde{Y}_n\tilde{u}_j)]}{\partial x_j}}_{\mathbf{IX}} - \underbrace{\frac{\partial (\bar{J}_{j,n} - \widetilde{J}_{j,n})}{\partial x_j}}_{\mathbf{X}} + \underbrace{\bar{\dot{\omega}}_n}_{\mathbf{XI}}$$

$$\bar{p} = \bar{\rho}R\widetilde{T} + \underbrace{\sum_{n=1}^{N} R_n\bar{\rho}(\widetilde{Y_n T} - \widetilde{Y}_n\widetilde{T})}_{\mathbf{XII}}$$

Filtered Navier-Stokes Equations

$$
\begin{aligned}
\frac{\partial(\bar{\rho}\widetilde{E})}{\partial t} + \frac{\partial[(\bar{\rho}\widetilde{E}+\bar{p})\tilde{u}_j]}{\partial x_j} - \frac{\partial(\tilde{\sigma}_{ij}\tilde{u}_i)}{\partial x_j} + \frac{\partial \tilde{q}_j}{\partial x_j} \quad = \quad & -\underbrace{\frac{\partial[\bar{\rho}(\widetilde{u_j h_s} - \tilde{u}_j\widetilde{h}_s)]}{\partial x_j}}_{\mathbf{III}} \\
& + \underbrace{\frac{\partial(\bar{\sigma}_{ij}\tilde{u}_i - \tilde{\sigma}_{ij}\tilde{u}_i)}{\partial x_j}}_{\mathbf{IV}} + \underbrace{\frac{\partial(\overline{u_i\sigma_{ij}} - \tilde{u}_i\bar{\sigma}_{ij})}{\partial x_j}}_{\mathbf{V}} \\
& - \underbrace{\frac{1}{2}\frac{\partial[\bar{\rho}(\widetilde{u_j u_i u_i} - \bar{\rho}\tilde{u}_j\widetilde{u_i u_i})]}{\partial x_j}}_{\mathbf{VI}} + \underbrace{\frac{\partial(\bar{q}_j - \tilde{q}_j)}{\partial x_j}}_{\mathbf{VII}} \\
& - \underbrace{\frac{\partial[\sum_{n=1}^{N}\Delta h_{f,n}^0\bar{\rho}(\widetilde{Y_n u_j} - \widetilde{Y}_n\tilde{u}_j)]}{\partial x_j}}_{\mathbf{VIII}}
\end{aligned}
$$

Subfilter Scale Modelling and Closures

- Subfilter scale stresses (term **I**): $\tau_{ij} = -2\mu_t \left(\widetilde{S}_{ij} - \frac{1}{3}\delta_{ij}\widetilde{S}_{ll} \right) + \frac{2}{3}\delta_{ij}\bar{\rho}\tilde{k}$
  - eddy-viscosity models
  - Smagorinsky (1963) & Yoshizawa (1986) models
  - one-equation model

- Subfilter scale scalar transport (term **IX**):

$$\bar{\rho}(\widetilde{Y_n u_j} - \widetilde{Y}_n \tilde{u}_j) = -\frac{\mu_t}{Sc_t}\frac{\partial \widetilde{Y}_n}{\partial x_j}$$

- Subfilter scale enthalpy transport (term **III**):

$$\bar{\rho}(\widetilde{u_j h_s} - \tilde{u}_j \widetilde{h}_s) = -\frac{\mu_t}{Pr_t}\frac{\partial \widetilde{T}}{\partial x_j}$$

- Subfilter turbulent diffusion (term **VI**, Knight *et al.* , 1998):

$$\frac{\bar{\rho}(\widetilde{u_j u_i u_i} - \bar{\rho}\tilde{u}_j \widetilde{u_i u_i})}{2} = \tau_{ij}\tilde{u}_i$$

Subfilter Scale Stress Models

Smagorinsky & Yoshizawa Models

Smagorinsky eddy-viscosity model (1963):

$$\tau_{ij} - \frac{\delta_{ij}}{3}\tau_{kk} = -2\bar{\rho}\nu_t \widetilde{S}_{ij}\,, \quad \nu_t = C_s^2 \Delta^2 |\widetilde{S}|\,, \quad |\widetilde{S}| = (2\widetilde{S}_{ij}\widetilde{S}_{ij})^{1/2}\,, \quad C_s \approx 0.10\text{-}0.24$$

Yoshizawa model (1986):

$$\tau_{kk} = C_I 2\bar{\rho}\Delta^2 |\widetilde{S}|^2\,, \quad C_I \approx 0.09\text{-}0.005$$

One-Equation Model

Eddy-viscosity:

$$\nu_t = C_v \sqrt{k}\Delta\,, \qquad C_v \approx 0.086\text{-}0.09$$

$\tilde{k}$-equation:

$$\frac{\partial(\bar{\rho}\tilde{k})}{\partial t} + \frac{\partial(\bar{\rho}\tilde{k}\tilde{u}_i)}{\partial x_i} = P - \epsilon + \frac{\partial}{\partial x_k}\left(\bar{\rho}\frac{\nu_t}{Pr_t}\frac{\partial \tilde{k}}{\partial x_k}\right)$$

Turbulence-Chemistry Interaction Models

Modelling Approaches for Premixed Combustion

- Thickened Flame Model
  - Butler & O'Rourke, 1977; Colin *et al.* , 2000
  - power-law flame wrinkling model (Charlette *et al.* , 2002)
- Flame-Surface Density (FSD) Model
  - Hawkes & Cant, 2000, 2001; Tullis & Cant, 2003
- G-Equation Model
  - Williams, 1985; Kerstein& Williams, 1988; Peters, 2000; Pitsch & Duchamp de Lageneste, 2002
- Laminar Flamelet Models
  - models based on the flamelet concept
  - Bray *et al.* , 1985; Peters, 1999;

Computational Framework

Key Elements I:

- Finite-Volume Formulation
  - reliable, robust, & accurate spatial discretizations
- Block-Based Adaptive Mesh Refinement
  - body-fitted multi-block mesh
  - local anisotropic mesh refinement
- Parallel Implementation Via Domain Decomposition
  - efficient and scalable algorithm
- Low-Mach Number Local Preconditioning
  - Weiss & Smith (1995)

Computational Framework

Key Elements I:

- Finite-Volume Formulation
  - reliable, robust, & accurate spatial discretizations
- Block-Based Adaptive Mesh Refinement
  - body-fitted multi-block mesh
  - local anisotropic mesh refinement
- Parallel Implementation Via Domain Decomposition
  - efficient and scalable algorithm
- Low-Mach Number Local Preconditioning
  - Weiss & Smith (1995)

Computational Framework

Key Elements I:

- Finite-Volume Formulation
  - reliable, robust, & accurate spatial discretizations
- Block-Based Adaptive Mesh Refinement
  - body-fitted multi-block mesh
  - local anisotropic mesh refinement
- Parallel Implementation Via Domain Decomposition
  - efficient and scalable algorithm
- Low-Mach Number Local Preconditioning
  - Weiss & Smith (1995)

Computational Framework

Key Elements I:

- Finite-Volume Formulation
  - reliable, robust, & accurate spatial discretizations
- Block-Based Adaptive Mesh Refinement
  - body-fitted multi-block mesh
  - local anisotropic mesh refinement
- Parallel Implementation Via Domain Decomposition
  - efficient and scalable algorithm
- Low-Mach Number Local Preconditioning
  - Weiss & Smith (1995)

Computational Framework

Key Elements II:

- Parallel Implicit Time-Marching Scheme
  - Newton-Krylov-Schwarz (NKS) approach for steady combustion (Keys and co-researchers, 1998, 2001; Groth & Northrup, 2005)
  - dual-time-stepping approach for unsteady combustion
- Development for Laminar and RANS
  - Northrup & Groth, 2005; Gao & Groth, 2005

Computational Framework

Key Elements II:

- Parallel Implicit Time-Marching Scheme
  - Newton-Krylov-Schwarz (NKS) approach for steady combustion (Keys and co-researchers, 1998, 2001; Groth & Northrup, 2005)
  - dual-time-stepping approach for unsteady combustion
- Development for Laminar and RANS
  - Northrup & Groth, 2005; Gao & Groth, 2005

Non-Premixed Laminar Diffusion Flame

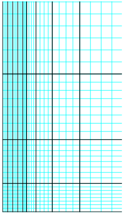

Inititial Level
96 Blocks (4x8)
3072 Cells

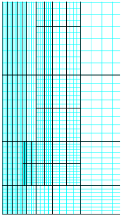

2 Levels of Refinement
126 Blocks (4x8)
4032 Cells

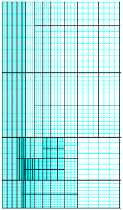

3 Levels of Refinement
195 Blocks (4x8)
6240 Cells

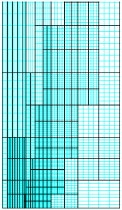

4 Levels of Refinement
327 Blocks (4x8)
10464 Cells

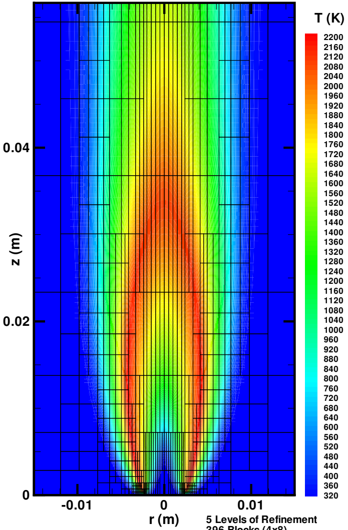

5 Levels of Refinement
396 Blocks (4x8)
12672 Cells

Non-Premixed Laminar Diffusion Flame

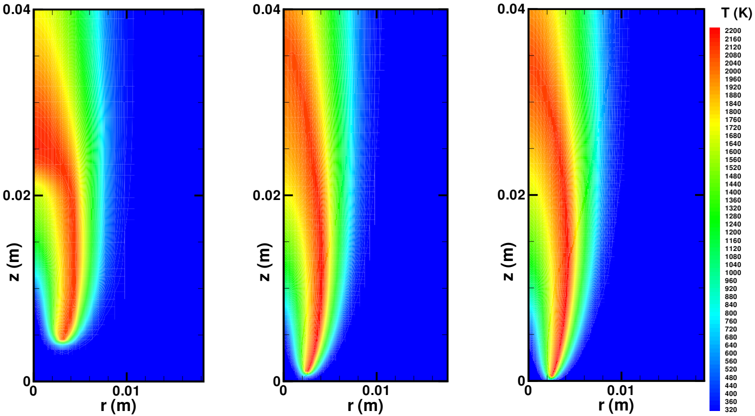

Initial Level - 96 Blocks(4x8)
3072 Cells

3rd Level - 195 Blocks (4x8)
6240 Cells

5th Level - 396 Blocks (4x8)
12672 Cells

5 refinements, 5 levels of refinement, 396 (4x8) blocks = 12672 cells

Non-Premixed Laminar Diffusion Flame

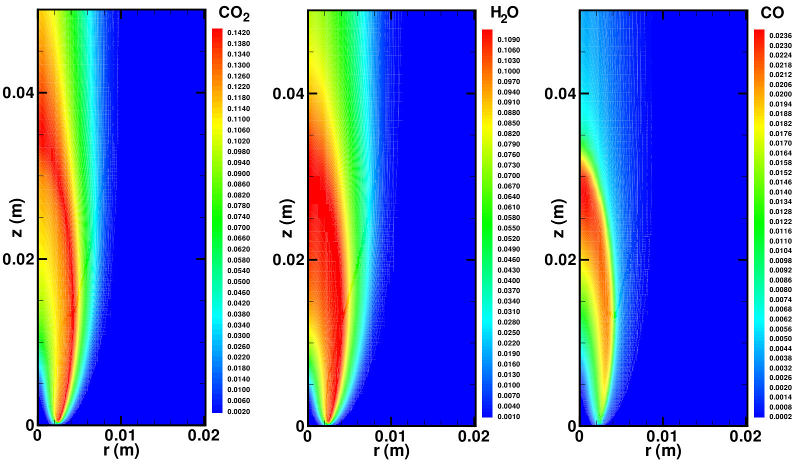

5 refinements, 5 levels of refinement, 396 (4x8) blocks = 12672 cells

Newton-Krylov Convergence

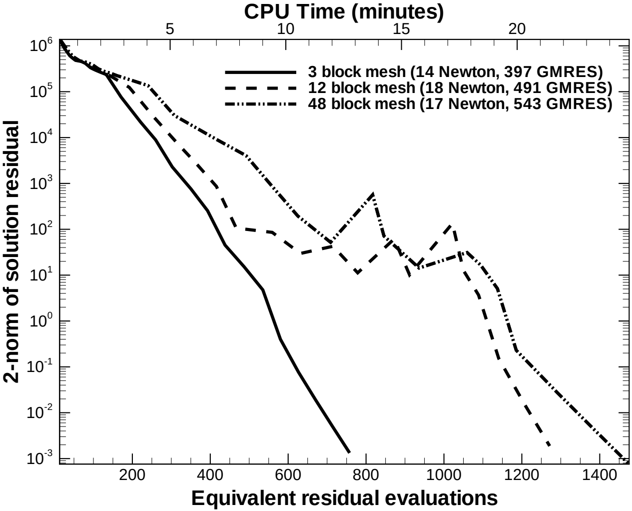

Non-Premixed Laminar Diffusion Flame

Parallel Performance with 96 blocks

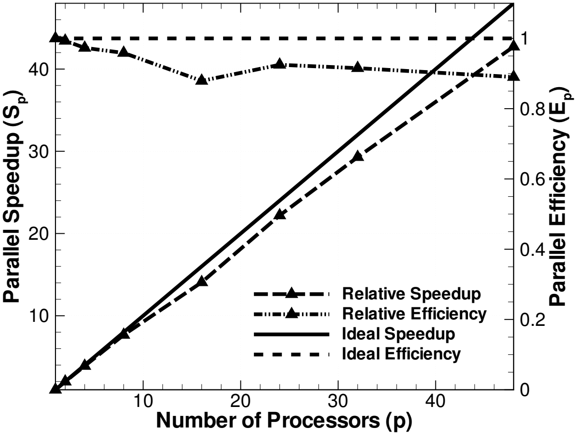

Parallel Speedup $S_p = t_1/t_p$, Parallel Efficiency $E_p = S_p/p$

Improved LES Capabilities

Grid-Independent LES

- explicit discrete filtering, adaptive mesh refinement (AMR)
- allow assessment and validation of subfilter scale models

High-Order Finite Volume Schemes

- high-order central essentially non-oscillatory (CENO) solution reconstruction (Ivan & Groth, 2006)
- parallel implementation with AMR

Least-Squares Discrete LES Filters

- high-order commutative discrete filters based on least-squares solution reconstruction

Thickened Flame Model

Modified Species Transport Equations

$$\frac{\partial(\bar{\rho}\widetilde{Y}_n)}{\partial t} + \frac{\partial(\bar{\rho}\widetilde{Y}_n\tilde{u}_j)}{\partial x_j} = -\frac{\partial(EF\widetilde{J}_{j,n})}{\partial x_j} - \frac{\partial[EF\bar{\rho}(\widetilde{Y_n u_j} - \widetilde{Y}_n\tilde{u}_j)]}{\partial x_j} + \frac{E\bar{\dot{\omega}}_n}{F}$$

$$D \rightarrow FED, \quad \mu \rightarrow FE\mu, \quad \dot{\omega} \rightarrow E\dot{\omega}/F$$

Power-Law Flame Wrinkling Model

$$\frac{s_{T\Delta}}{s_l^0} = \frac{A_{\text{sfs}}}{\Delta^2} = \Xi_\Delta = \left(1 + \frac{\Delta}{\eta_c}\right)^\beta = E \;, \;\; \eta_c = \mid \langle \nabla \cdot \mathbf{n}_s \rangle \mid^{-1}$$

where E is the efficiency factor, Ξ_Δ is the subfilter wrinkling factor, and η_c is an inner cutoff scale

Thickened Flame Model

Efficiency Function (Charlette *et al.* , 2002)

$$| \langle \nabla \cdot \mathbf{n} \rangle_s | = \Delta^{-1} \frac{u'_\Delta}{s_l^0} \Gamma \left(\frac{\Delta}{\delta_l^0}, \frac{u'_\Delta}{s_l^0}, Re_\Delta \right)$$

$$\Gamma \left(\frac{\Delta}{\delta_l^0}, \frac{u'_\Delta}{s_l^0}, Re_\Delta \right) = \{ [(f_u^{-a} + f_\Delta^{-a})^{-1/a}]^{-b} + f_{Re}^{-b} \}^{-1/b} ,$$

Thickened Flame Structure

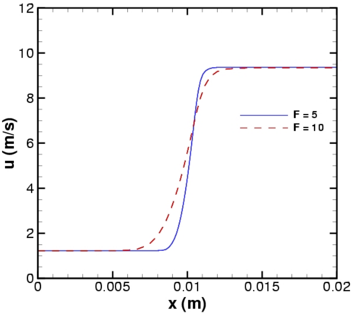

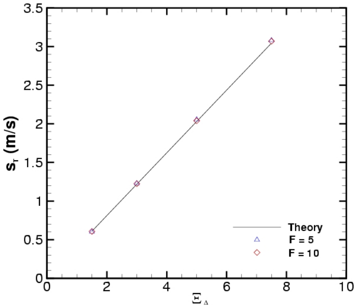

Freely Propagating Methane/Air Flame

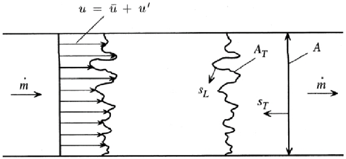

Chemical Kinetic & Thermodynamic/Trasport Models

- 2-step 6-species reduced chemical kinetic scheme (Westbrook & Dryer, 1981):

$$2\,\mathrm{CH_4} + 3\,\mathrm{O_2} \rightleftharpoons 2\,\mathrm{CO} + 4\,\mathrm{H_2O}$$

$$2\,\mathrm{CO} + \mathrm{O_2} \rightleftharpoons 2\,\mathrm{CO_2}$$

- thermodynamic & transport properties (Gordon & McBride, 1994, 1996)
- mixture viscosity and thermal conductivity rules of Wilke (1950) and Mason & Saxena (1964)

Thickened-Flame/Powerlaw-Flame-Wrinkling Model Solutions

Parameters Characterizing Premixed Flame:

$\phi = 1$, $\bar{u} = s_l^0$, $u' = 2.53$ m/s, $\ell = 7.3$ mm, $\lambda = 1.34$ mm, $Re_\ell = 1164$, $Re_\lambda = 213$, $s_l^0 = 0.406$ m/s, and $\delta_l^0 = 0.27$ mm.

Calculations Performed in Three Steps:

- 1D laminar flame solution
- Wrinkling of the flame front by 2D homogenous turbulence without reactions (Rogallo, 1981)
- 2D wrinkled flame front with reactions

CH_4, $F = 10$ | CH_4, $F = 5$

CO, $F = 10$ | CO, $F = 5$

Predicted Turbulent Flame Structure

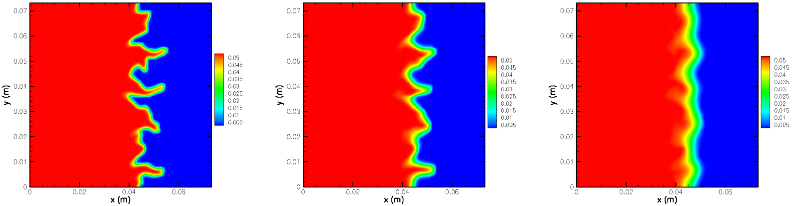

- Distributions of CH_4 mass fraction at t = 0.98 ms (after 2.8 eddy turnover times)
- F = 5, 10, 20

Predicted Turbulent Flame Structure

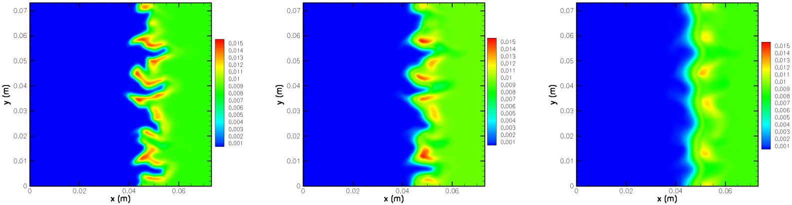

- Distributions of CO mass fraction at t = 0.98 ms (after 2.8 eddy turnover times)
- CO enhancement in positive cusps (Echekki & Chen, 1996; Hawkes & Chen, 2004)

Predicted Turbulent Burning Rate

Rate of consumption of methane: $s_t = \frac{1}{\rho_0 Y_0 L_y} \int_A \bar{\dot{\omega}}_F dA$

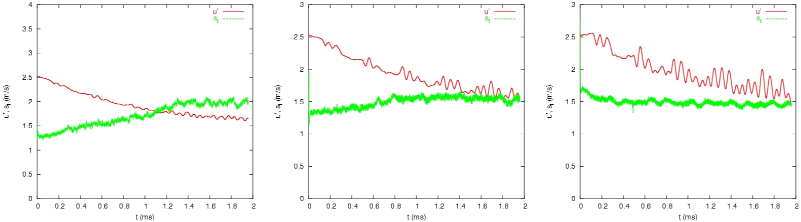

Burning rate, F = 5, 10, 20

Gülder expression (1990)	Average burning rate (F=10)
1.5 m/s	1.544 m/s

Predicted Turbulent Burning Rate

Rate of consumption of methane: $s_t = \frac{1}{\rho_0 Y_0 L_y} \int_A \bar{\dot{\omega}}_F dA$

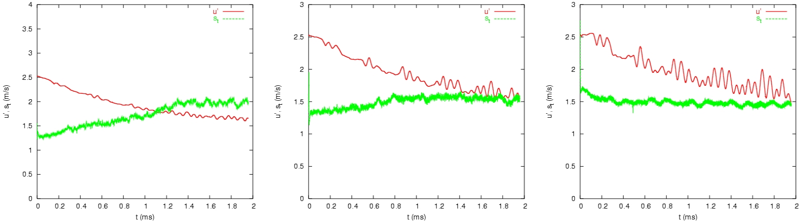

Burning rate, F = 5, 10, 20

Gülder expression (1990)	Average burning rate (F=10)
1.5 m/s	1.544 m/s

Predicted Turbulent Flame Structure Using AMR

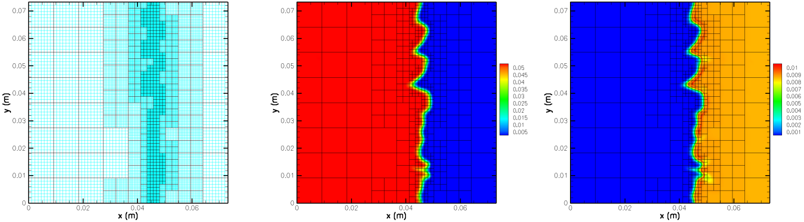

- Computational mesh and distributions of CH_4 and CO mass fractions at t = 0.245 ms
- 4 levels of mesh refinement, 8×8 solution blocks, 600-700 blocks

Flame Surface Density (FSD) SFS Model

The flame surface density (FSD) model of Hawkes and Cant (2000, 2001) is being developed for predicting premixed combustion via LES

$$c = \frac{T - T_u}{T_b - T_u} \quad \text{or} \quad c = \frac{Y_F - Y_F^u}{Y_F^b - Y_F^u} \qquad 0 \leq c \leq 1$$

$$\frac{\partial}{\partial t}\left(\rho\tilde{c}\right)+\frac{\partial}{\partial x_i}\left(\rho\tilde{u}_i\tilde{c}\right)+\frac{\partial}{\partial x_i}\rho\left(\widetilde{u_i c}-\tilde{u}_i\tilde{c}\right)=\frac{\partial}{\partial x_i}\left(\overline{\rho D\frac{\partial c}{\partial x_i}}\right)+\bar{\dot{\omega}}_c=\overline{\rho s_d|\nabla c|}$$

$$\overline{\rho s_d|\nabla c|} \approx \rho_u s_L \Sigma$$

$$\frac{\partial\Sigma}{\partial t}+\frac{\partial}{\partial x_i}\left(\tilde{u}_i\Sigma\right)=-\frac{\partial}{\partial x_i}\left(\overline{(u_i)_s'\Sigma}\right)+\left(S_{mean}+S_{hr}+S_{sg}\right)\Sigma+P_{mean}+P_{sg}$$

G-Equation SFS Model

A G-equation approach is being developed for predicting premixed combustion via LES. Assumes thin flame surface and flame-front position is represented with a constant value of the level set function, G (Williams, 1985; Kerstein& Williams, 1988; Peters, 2000; Pitsch & Duchamp de Lageneste, 2002).

$$\frac{\partial(\bar{\rho}\widetilde{G})}{\partial t} + \frac{\partial(\bar{\rho}\tilde{u}_i\widetilde{G})}{\partial x_i} = \overline{\rho w|\nabla G|}$$

$$w = \bar{s}_T \qquad \frac{\bar{s}_T}{s_L} = 1 + \alpha\left(\frac{\bar{u}'}{s_L}\right)^q$$

Concluding Remarks

- Overview of numerical modelling of premixed combustion processes: motivation, numerical challenges, and approaches
- Described numerical results for thickened-flame/powerlaw-flame-wrinkling model
- Future Research
  - Moving to three-dimensional turbulence
  - Comparison of subfilter scale models
  - Use of high-order spatial and temporal discretizations
  - Use of explicit filtering based on high-order commutative discrete filters
  - Study of hydrogen enrichment of methane

Concluding Remarks

- Overview of numerical modelling of premixed combustion processes: motivation, numerical challenges, and approaches
- Described numerical results for thickened-flame/powerlaw-flame-wrinkling model
- Future Research
  - Moving to three-dimensional turbulence
  - Comparison of subfilter scale models
  - Use of high-order spatial and temporal discretizations
  - Use of explicit filtering based on high-order commutative discrete filters
  - Study of hydrogen enrichment of methane

Concluding Remarks

- Overview of numerical modelling of premixed combustion processes: motivation, numerical challenges, and approaches
- Described numerical results for thickened-flame/powerlaw-flame-wrinkling model
- Future Research
  - Moving to three-dimensional turbulence
  - Comparison of subfilter scale models
  - Use of high-order spatial and temporal discretizations
  - Use of explicit filtering based on high-order commutative discrete filters
  - Study of hydrogen enrichment of methane

Flame and Flow Parameters

- Axisymmetric Bunsen-type burner
  - nozzle diameter of 11.2mm
  - turbulence was generated by perforated plates 3-diameter lengths upstream of the burner nozzle.
- Methane/air mixtures were selected to provide:

Exit velocities	14.43, 14.62, 14.77 m/s
Turbulent intensities (u')	1.37, 1.41, 1.81 m/s
Equivalence ratios (ϕ)	0.6, 0.7, 0.8, 0.9, 1.0
Non-dimensional turbulent intensities (u'/S_L)	3.4 - 15.3

Planar Rayleigh Scattering Setup

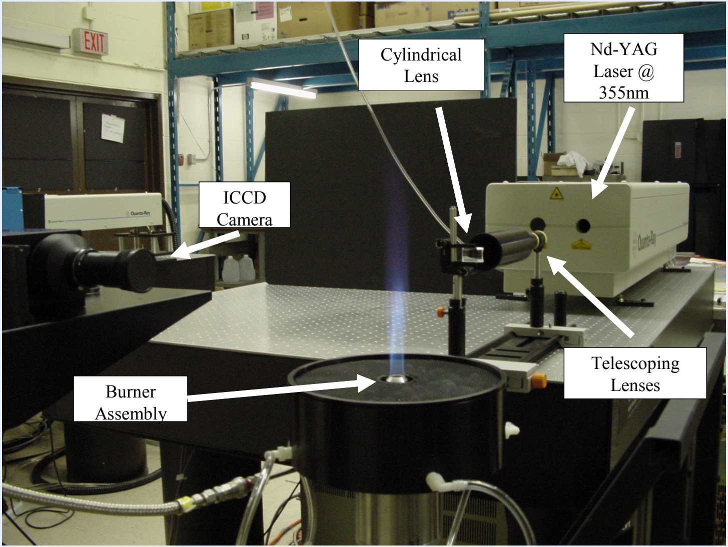

Planar Rayleigh Scattering Setup

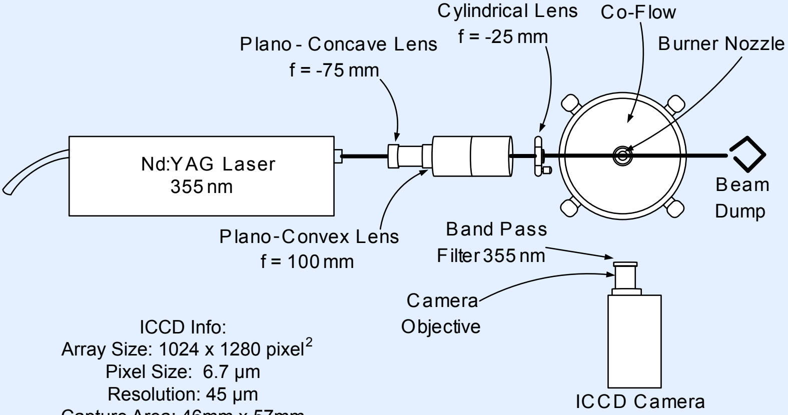

ICCD Info:
Array Size: 1024 x 1280 pixel^2
Pixel Size: 6.7 μm
Resolution: 45 μm
Capture Area: 46mm x 57mm

Flame Front Temperature

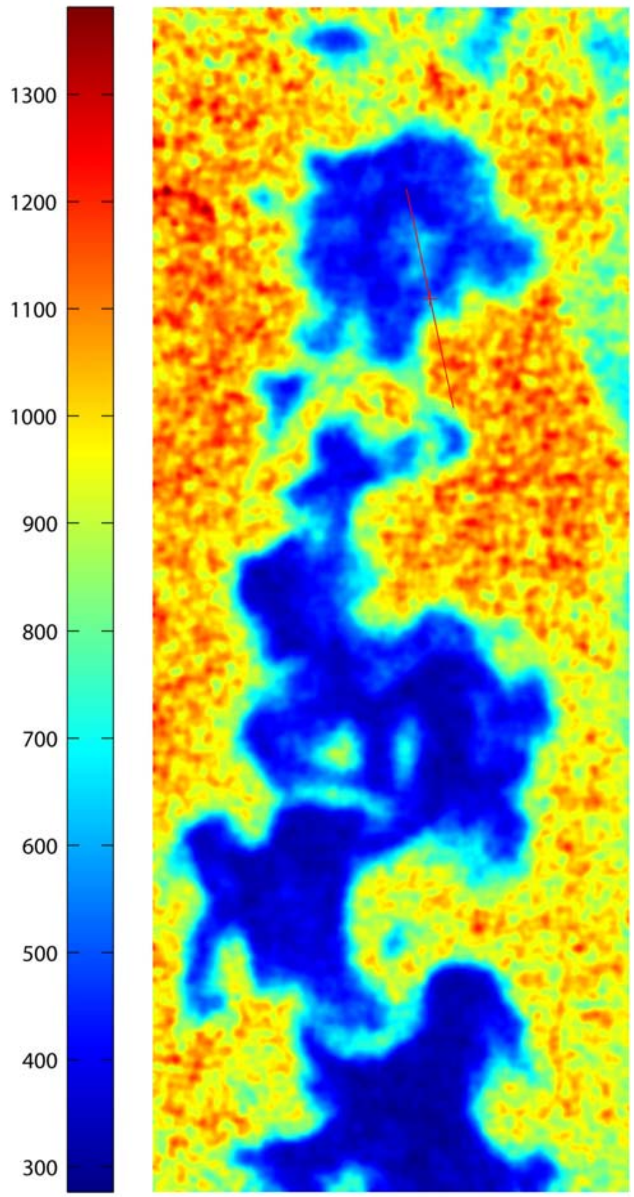

Rayleigh scattering; CH_4-air

$\Phi = 0.7$; $u'/S_{\mathrm{L}} = 15$

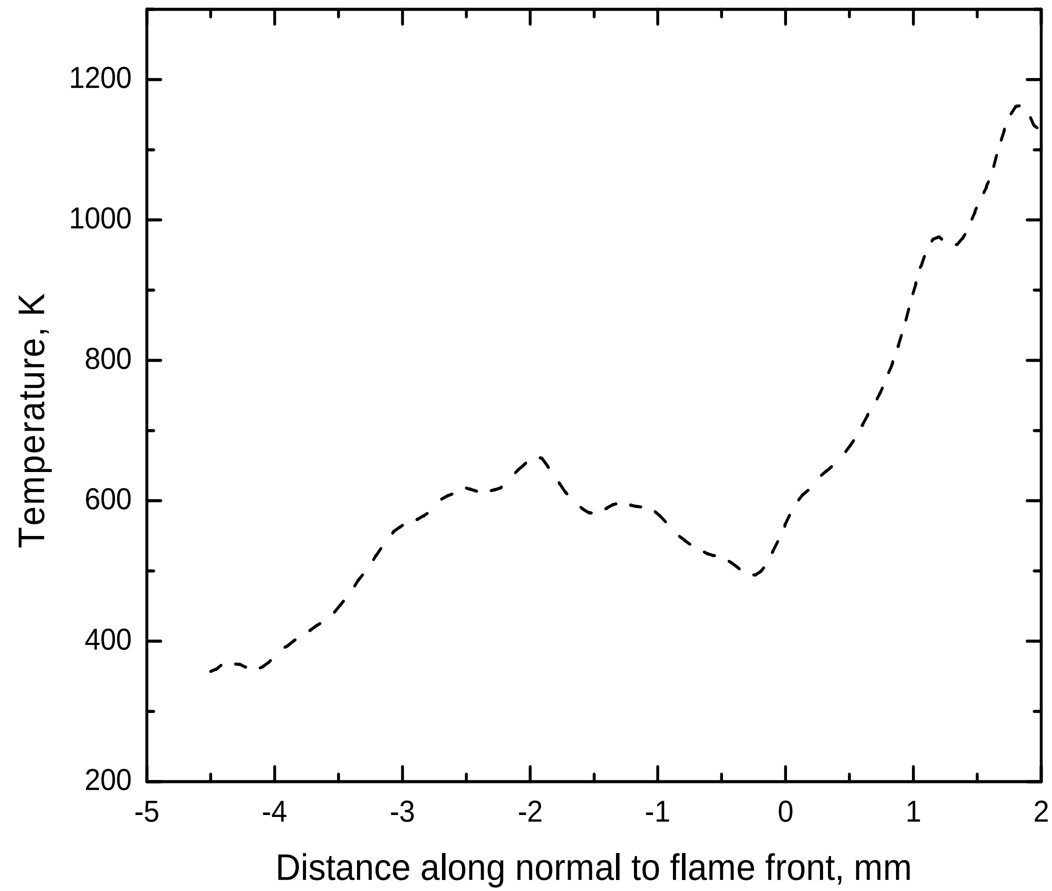

Flame Front Temperature

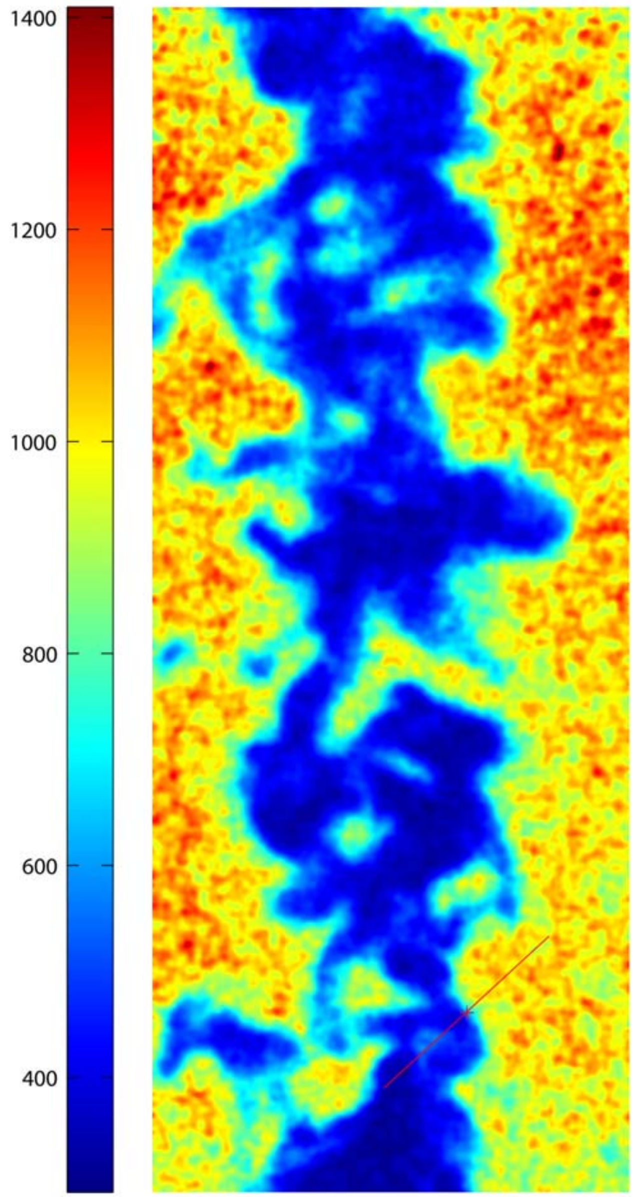

Rayleigh scattering; CH_4-air

$\Phi = 0.7;\ u'/S_{\mathrm{L}} = 15$

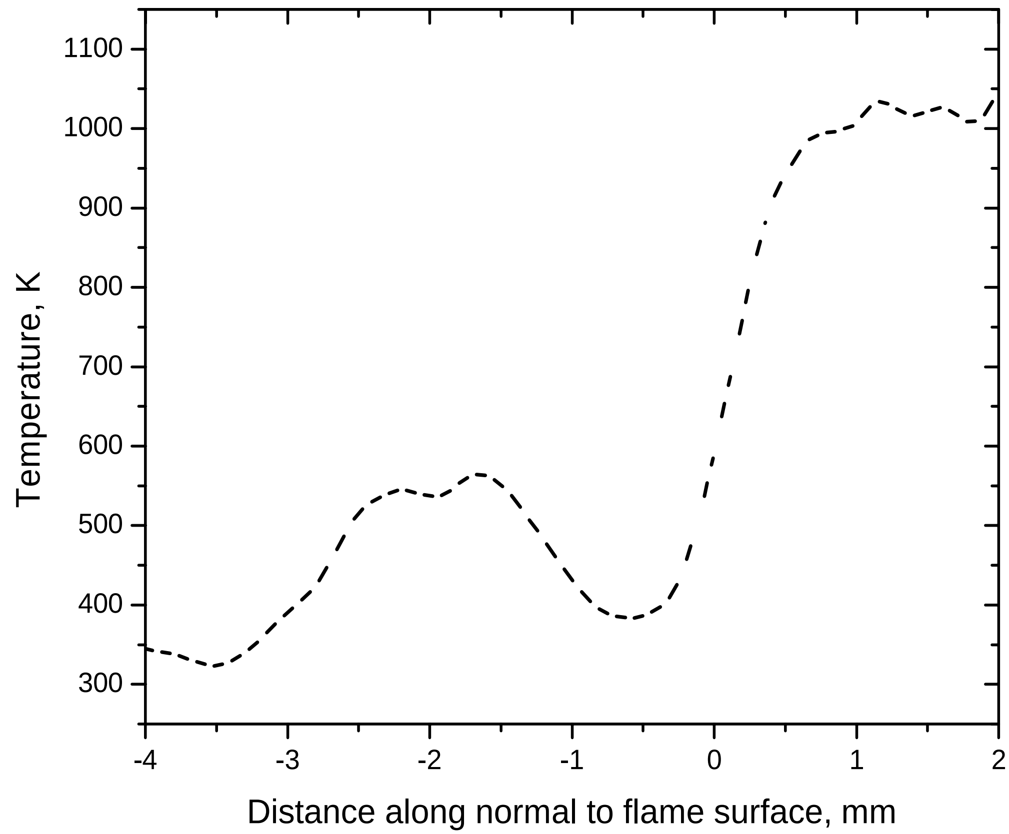

University of Toronto
Institute for Aerospace Studies
Combustion & Propulsion Group

Flame Front Temperature

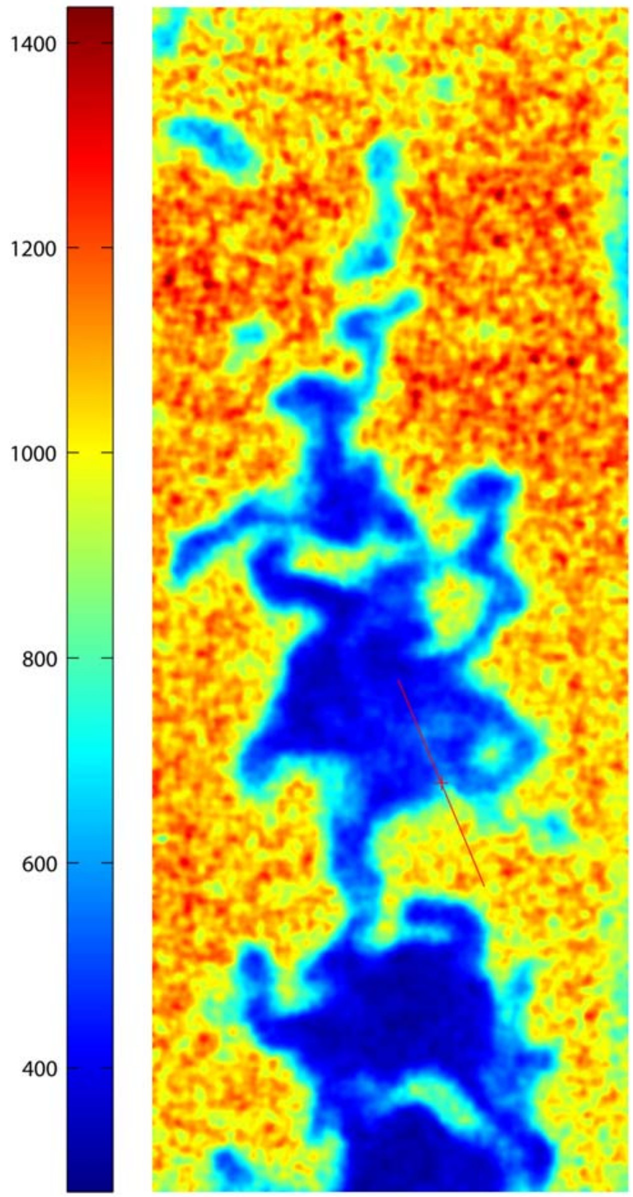

Rayleigh scattering; CH_4-air

$\Phi = 0.7$; $u'/S_{\mathrm{L}} = 15$

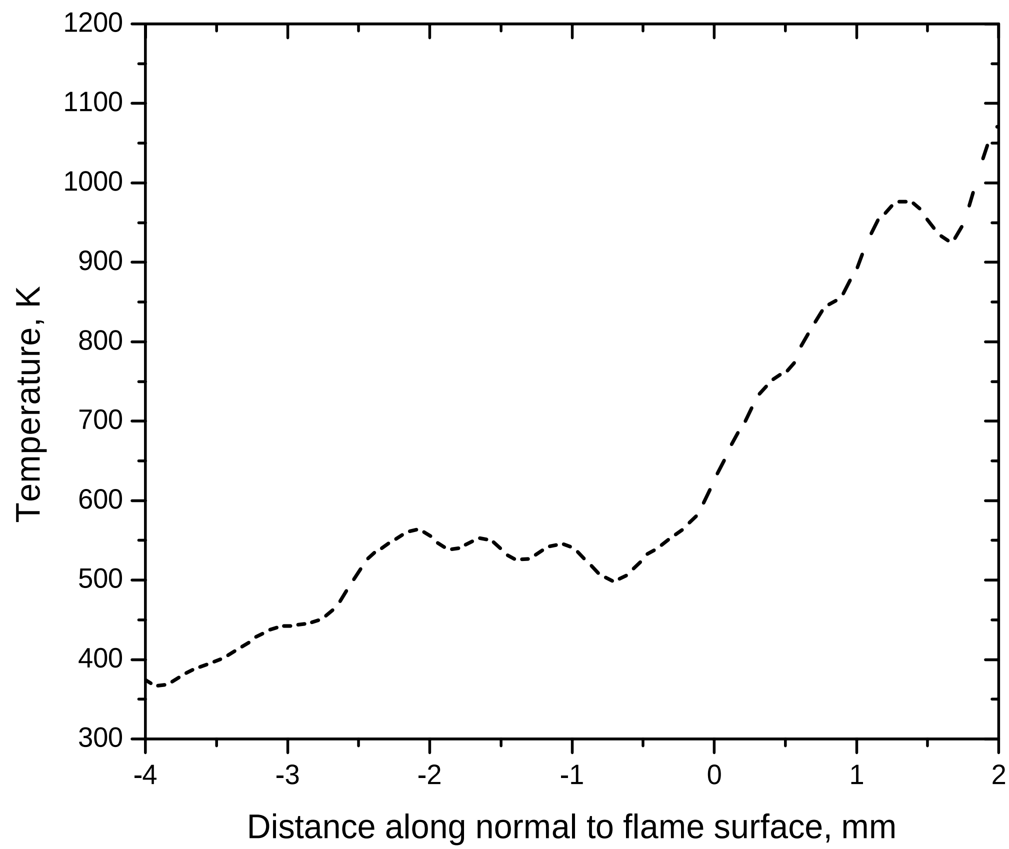

Averaged Temperature Profiles

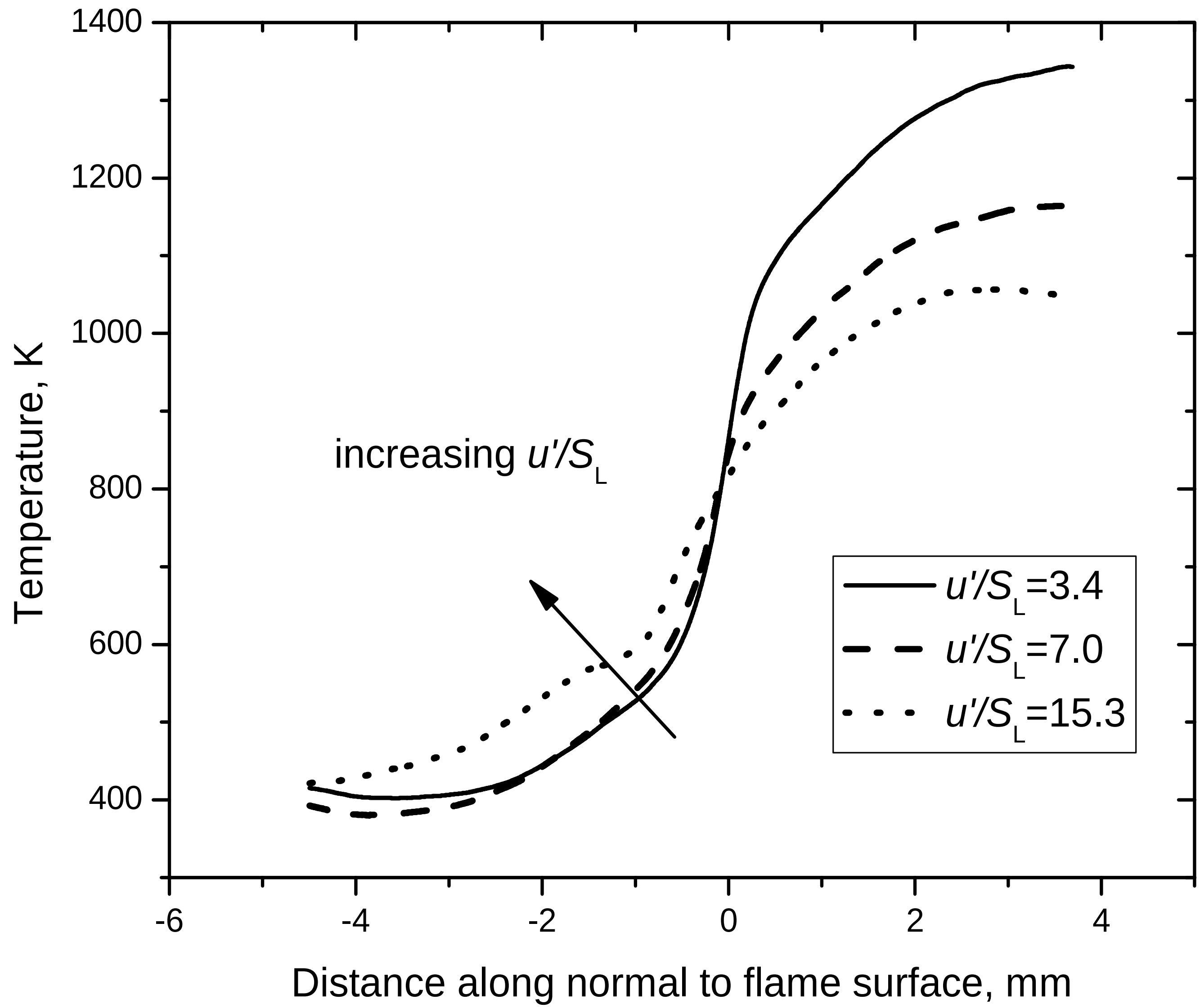

Effects of Non-Dimensional Turbulent Intensities

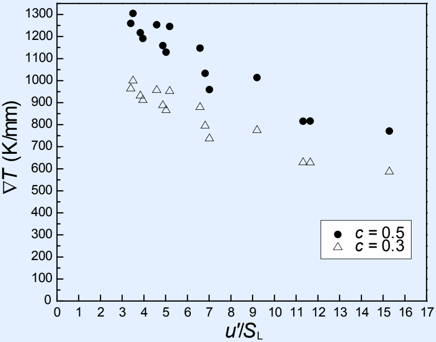

Variation of Gradients with u'/S_L

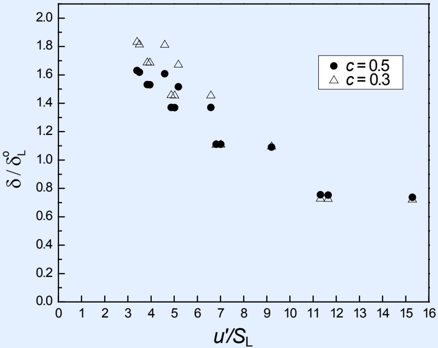

Normalized flame front thicknesses by unstretched laminar flame thickness (δ_L^o) at different u'/S_L

Effect of Equivalence Ratio

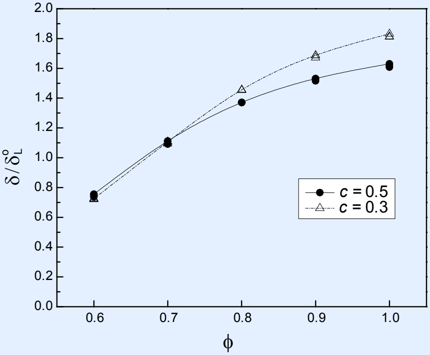

Normalized flame front thickness as a function of equivalence ratio (ϕ)

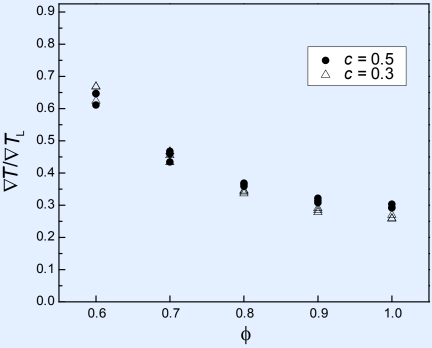

Normalized temperature gradients as a function of equivalence ratio (ϕ)

NRC-CNRC

Institute for Chemical Process and Environmental Technology

Flammability Limit and NO_X Formation of Fuel Enriched Lean Premixed Flames

Hongsheng Guo, Gregory J. Smallwood
National Research Council Canada
Ottawa, Ontario K1A 0R6

Background

- Lean premixed combustion is a promising concept for significantly improving fuel conversion efficiency and reducing pollutant emissions;
- Lean premixed flames are less stable, due to the narrow flammable range at leaner condition;
- Hydrogen enrichment can enlarge the flammable range of lean premixed flames, and thus improve flame stability;
- Hydrogen can be obtained by fuel reforming;
- A reformate gas contains not only hydrogen, but also carbon monoxide and other components;
- ***Will reformate gas enrichment be helpful?***

Objectives

- Investigate the effect of reformate gas enrichment on extinction characteristics of CH_4/air premixed flames;
- Study the mechanisms of NO_X formation in reformate gas enriched CH_4/air lean premixed flames.

Flame Configuration

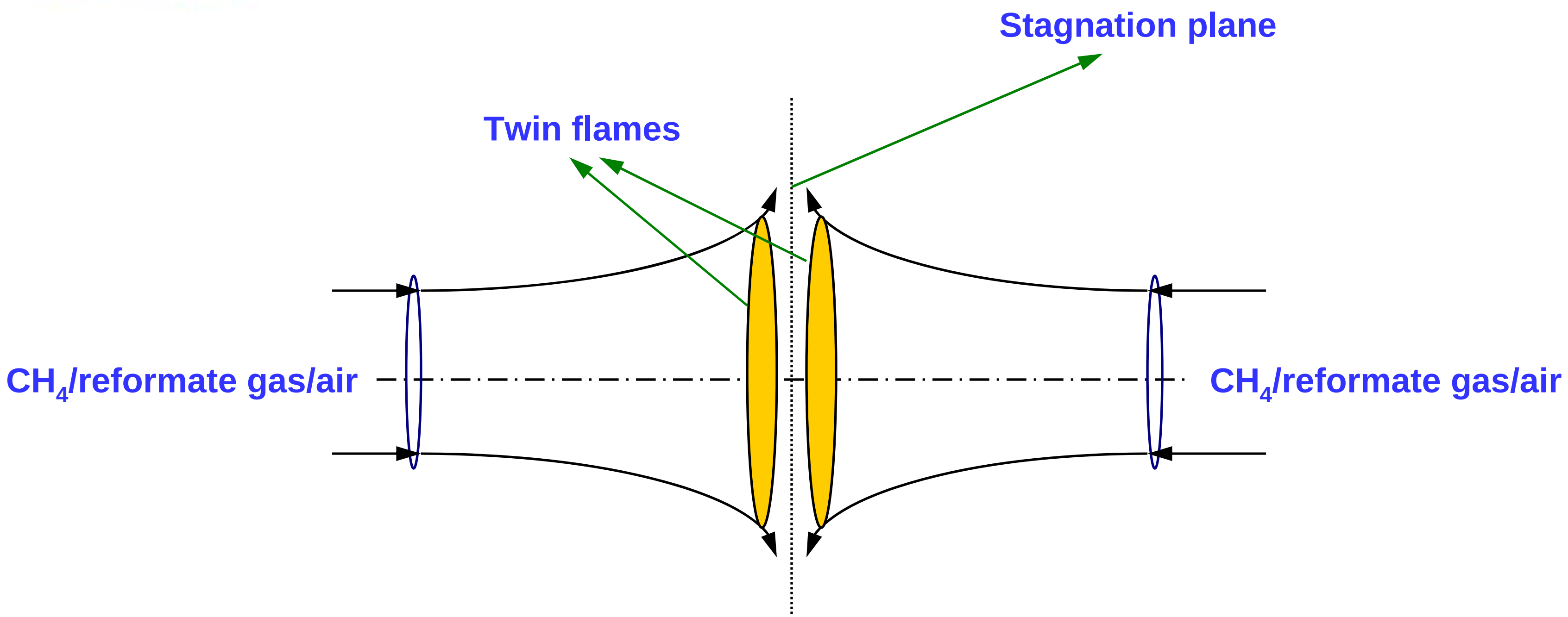

Numerical Model

- Potential boundary conditions;
- Adaptive refinement of meshes;
- Atmosphere pressure, and room temperature, 300 K;
- Radiation: optically thin model;
- Reaction scheme: Gri-Mech 3.0;
- Reformate gases: partial oxidation of CH_4

$$2CH_4 + O_2 + \gamma N_2 = 2CO + 4H_2 + \gamma N_2$$

$\gamma = 0$	---	reformate gas 1
$\gamma = 3.76$	---	reformate gas 2

Enrichment fraction: $\alpha_{rg} = V_{rg}/(V_{rg}+V_{CH4})$

NRC·CNRC
Institute for Chemical Process and Environmental Technology

Extinction Limits of Pure CH_4/Air Flames

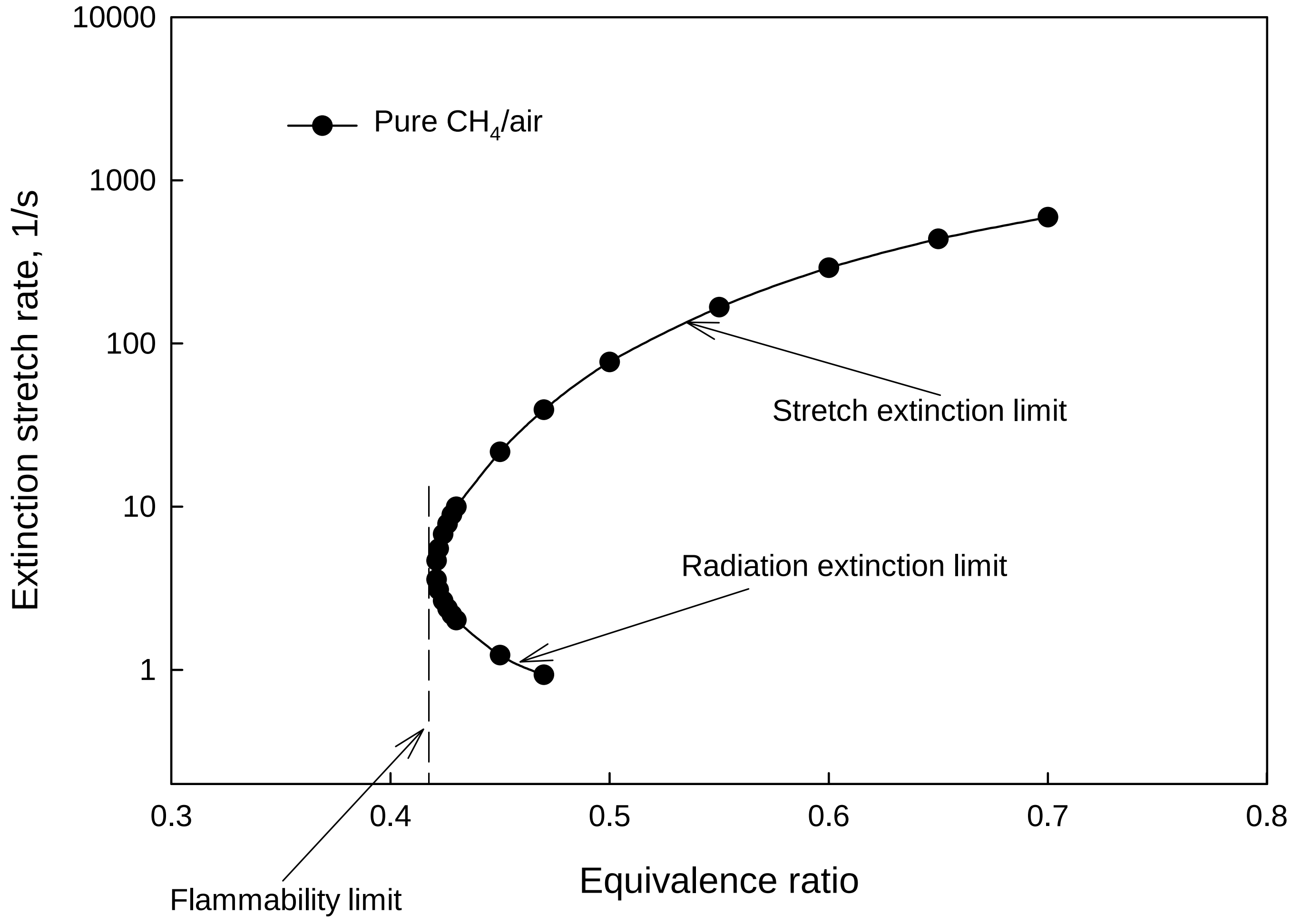

NRC·CNRC
Institute for Chemical Process and Environmental Technology

Extinction Limits

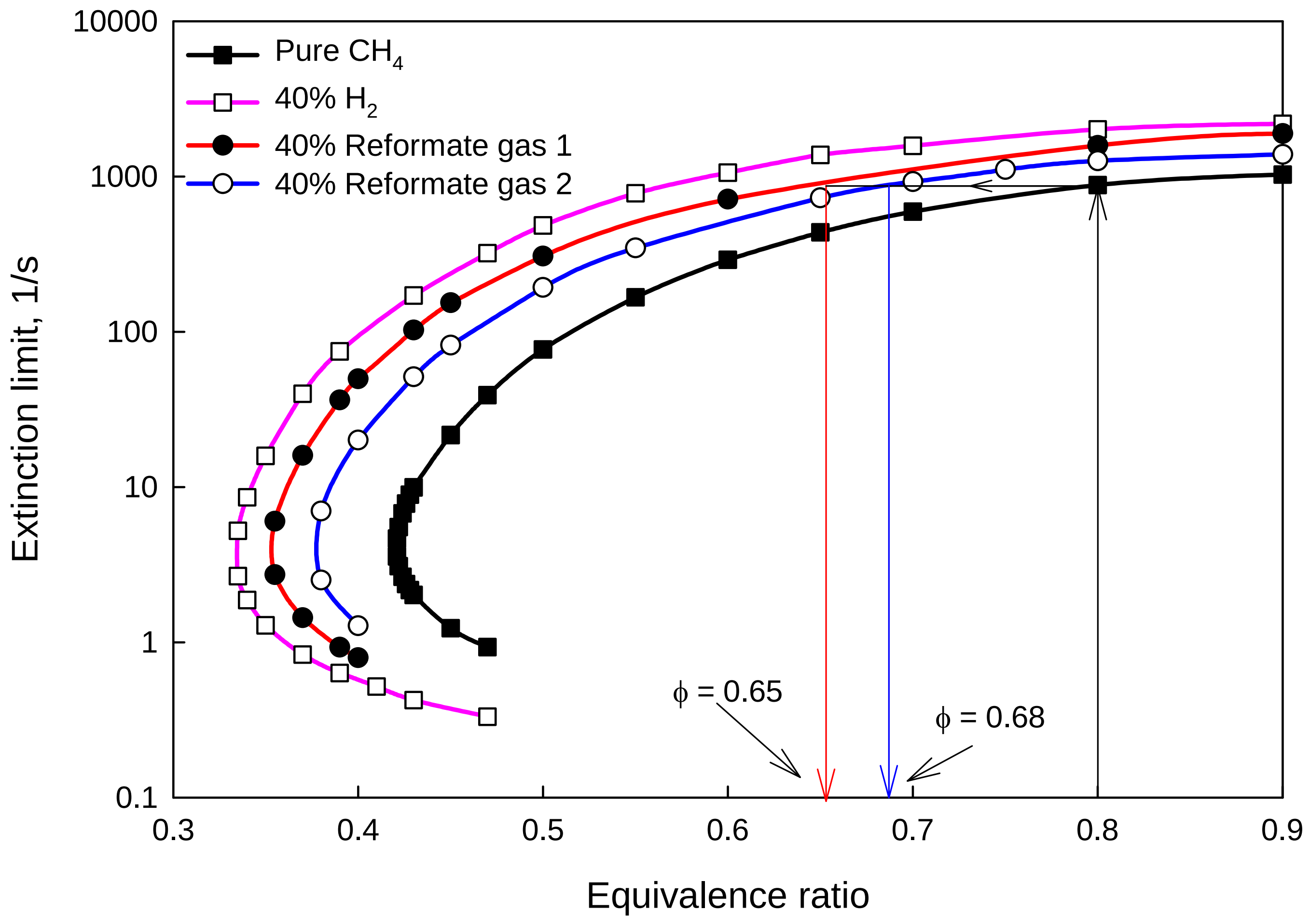

The addition of a reformate gas does enlarge the flammable range and lower the flammability limit.

NO Formation

$\phi = 0.65$

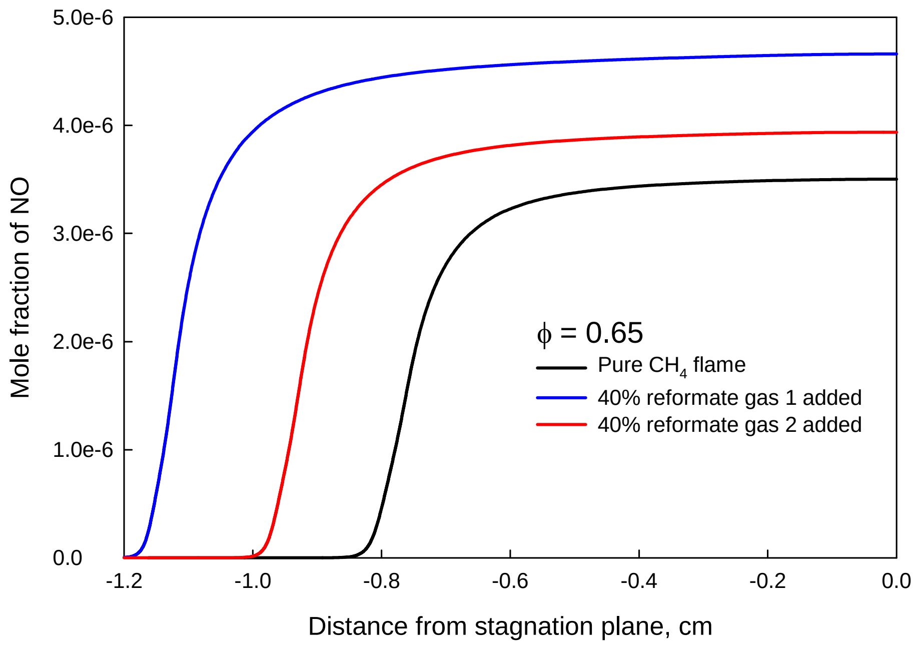

$\phi = 0.9$

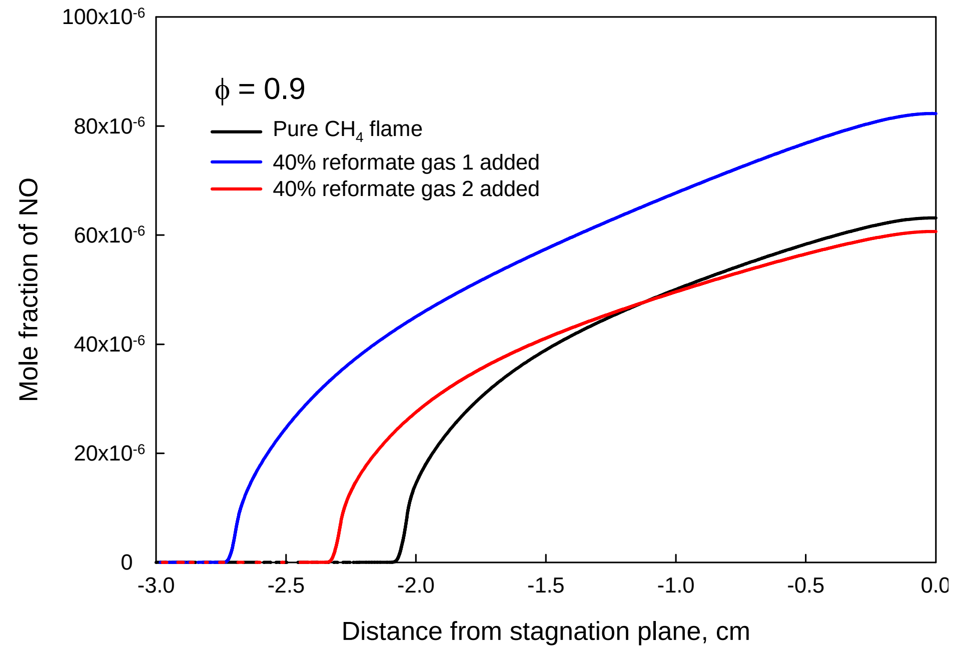

- **The addition of reformate gas 1 always increases the formation of NO;**
- **The effect of reformate gas 2 addition on NO formation depends on equivalence ratio, because of the variation in flame temperature.**

Flame Temperature

ϕ = 0.65

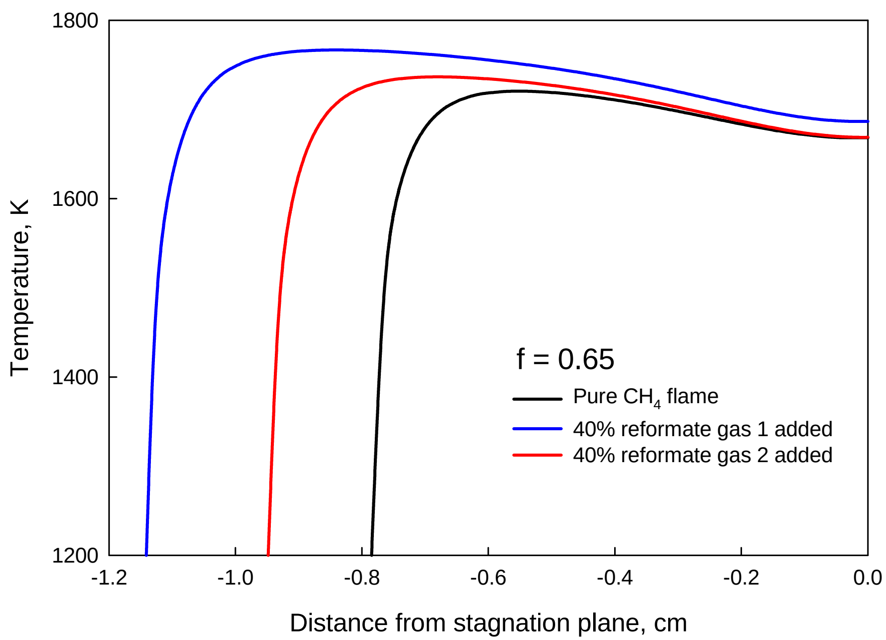

ϕ = 0.9

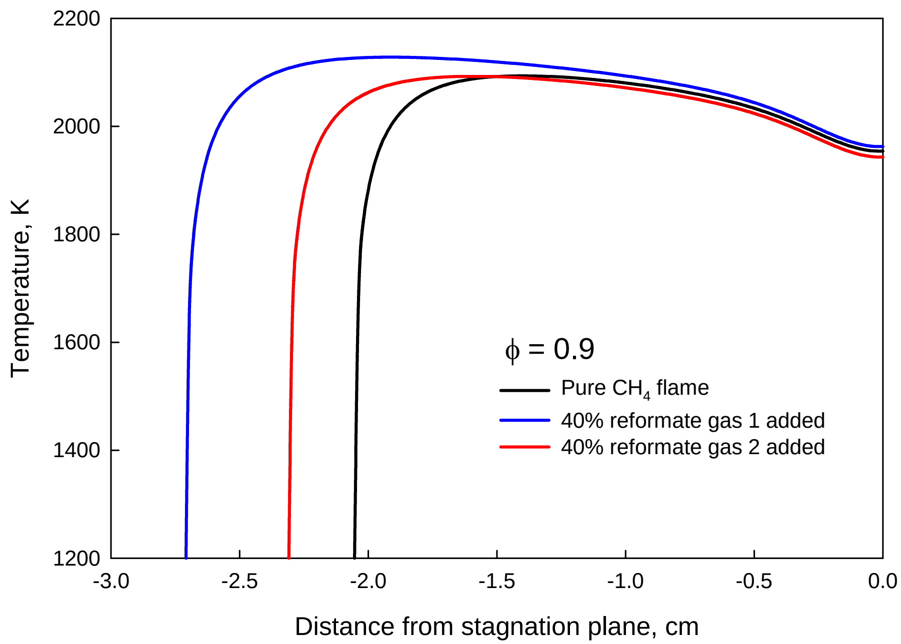

NRC-CNRC
Institute for Chemical Process and Environmental Technology

Variation of NO Formation Mechanism (ϕ = 0.9, reformate gas 2)

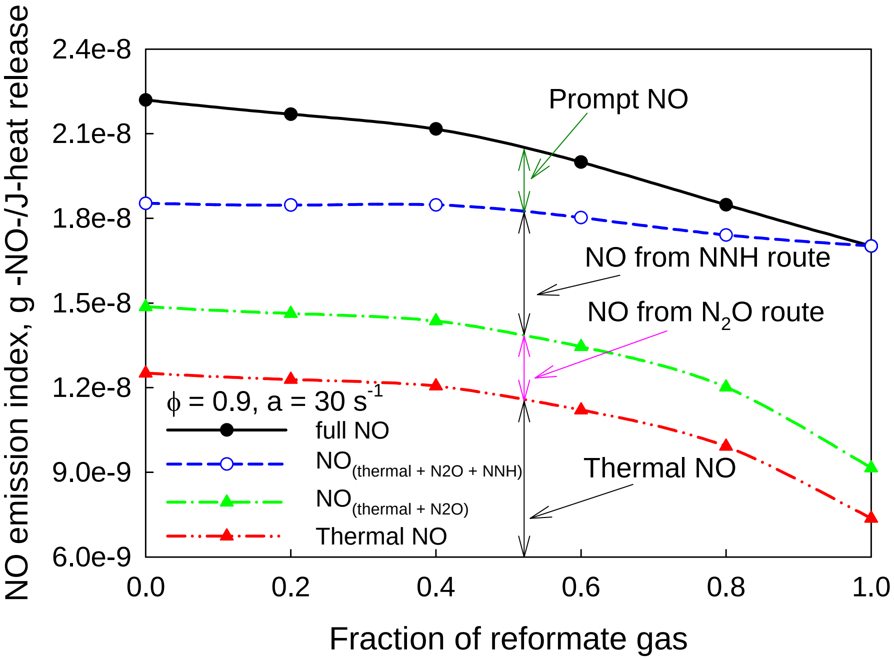

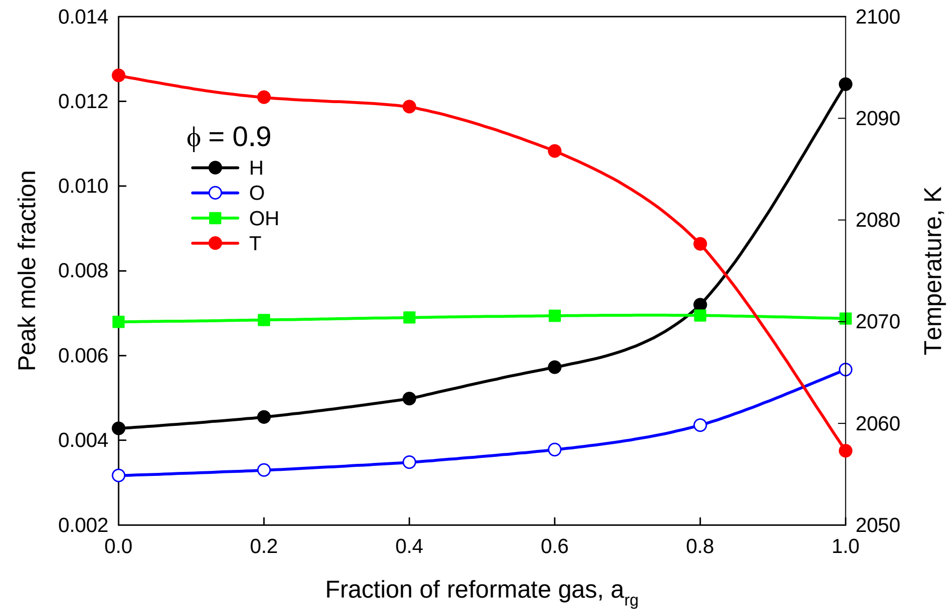

- The addition of reformate gas reduces the contributions of the prompt and thermal routes, because of the decrease in CH concentration and flame temperature;
- The contribution of the NNH intermediate route increases, because: $NNH = N_2 + H$, $OH + H_2 = H_2O + H$, $CO + OH = H + CO_2$.

Variation of NO Formation Mechanism (ϕ = 0.65, reformate gas 2)

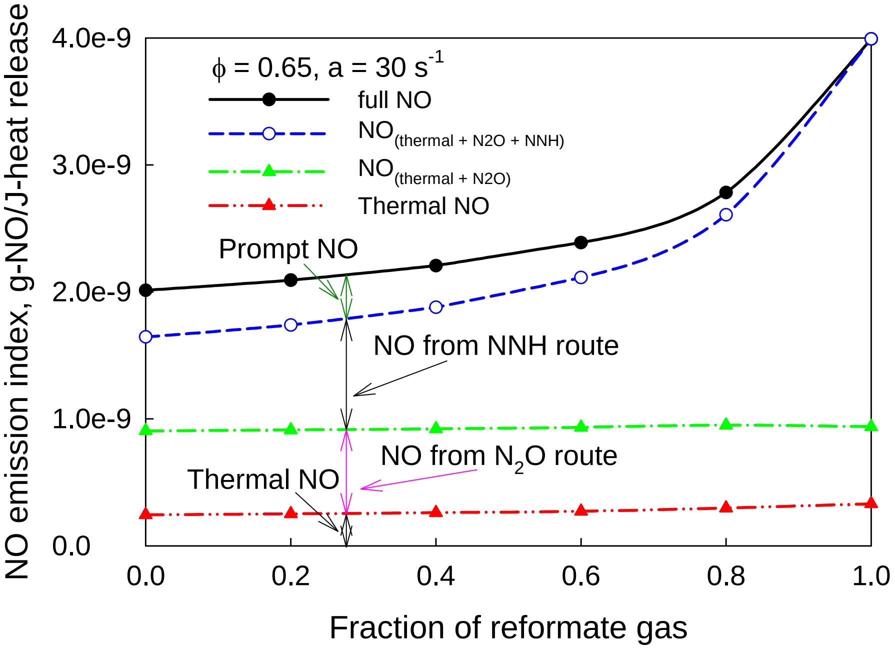

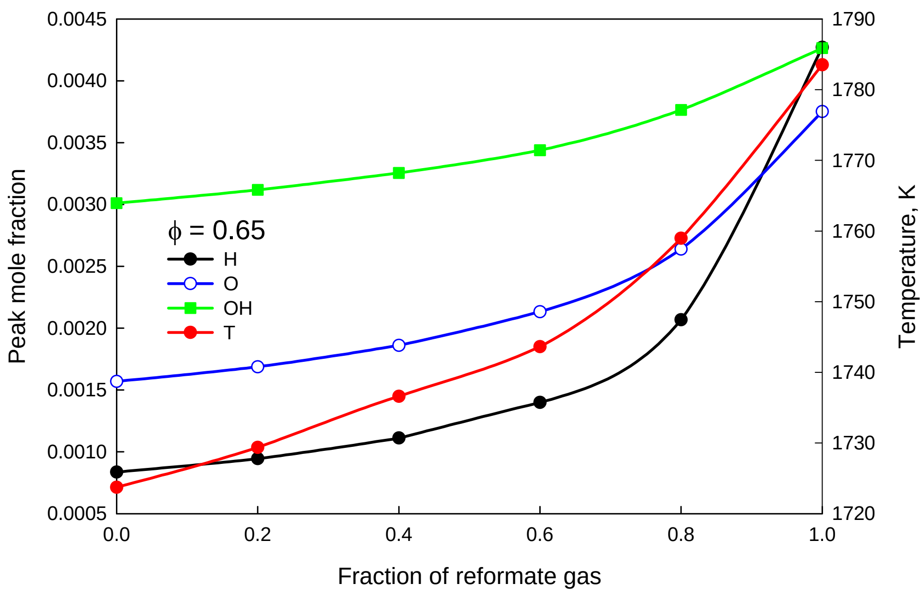

- Reformate gas addition significantly increases the contribution of the NNH route and slightly increases that of the thermal route;
- But reformate gas addition reduces the contribution of the prompt route.

NRC·CNRC
Institute for Chemical Process and Environmental Technology

NO Formation

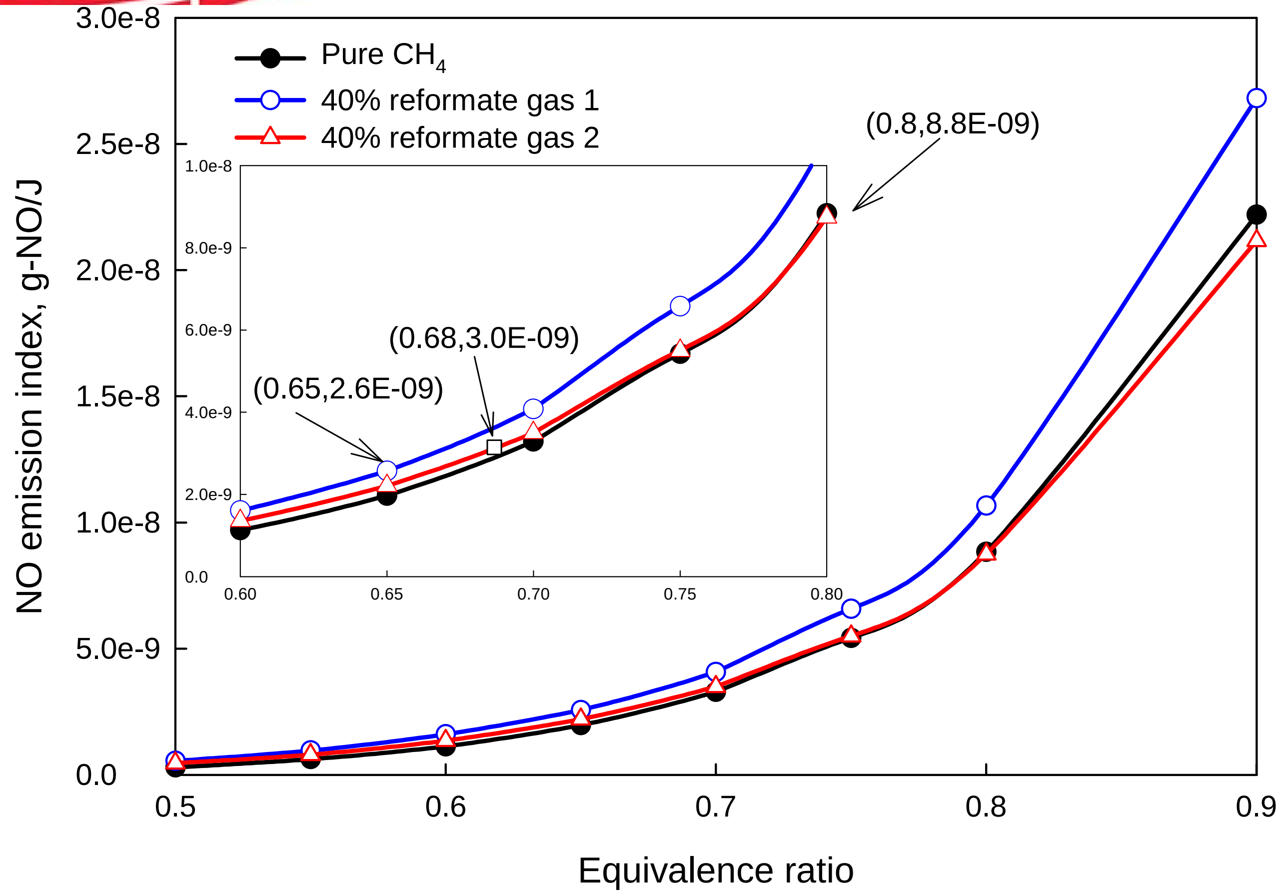

- **The formation of NO can be significantly reduced in a reformated gas enriched flame, by operating under leaner condition.**

NO_2 Formation

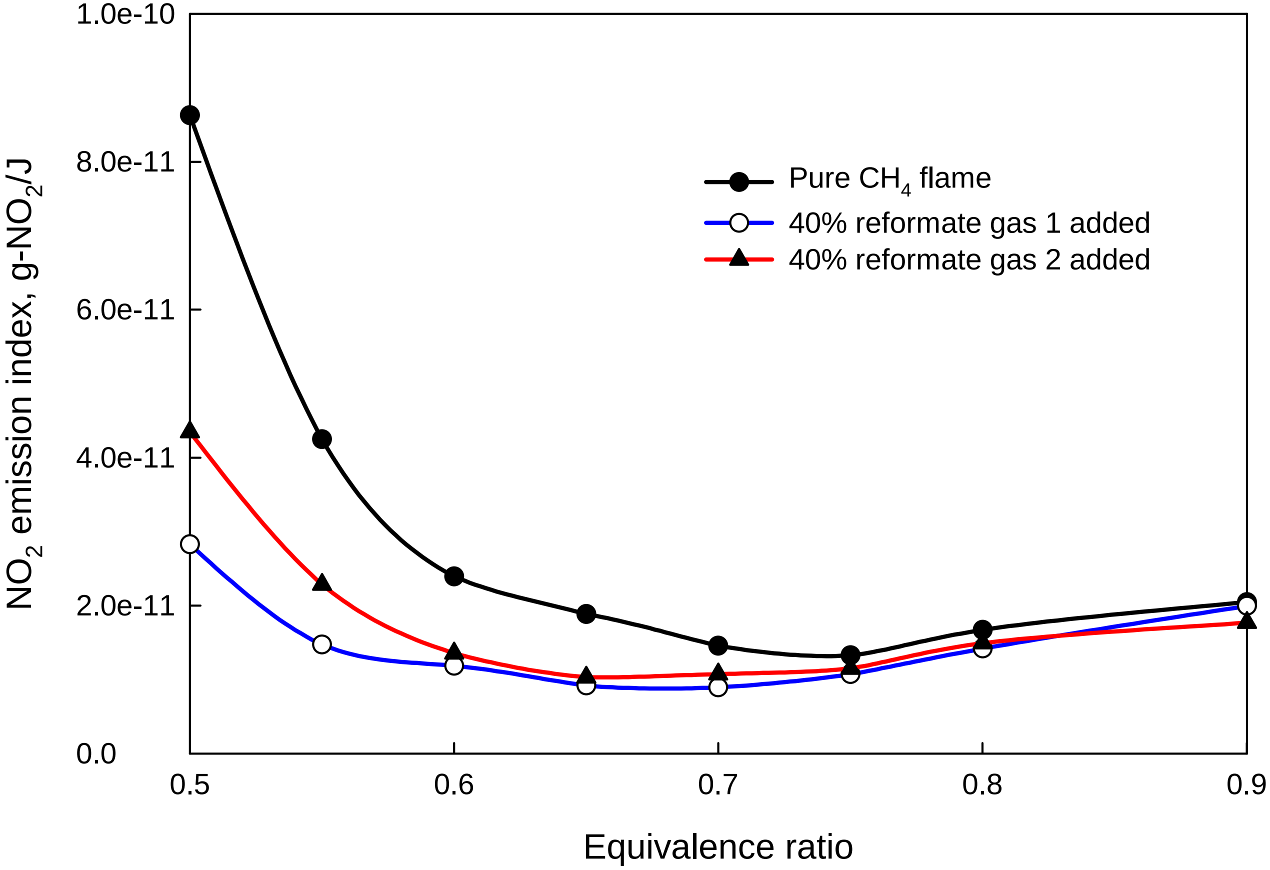

- $HO_2 + NO = NO_2 + OH$
- $NO_2 + H = NO + OH$

- **At a lower equivalence ratio, the addition of a reformate gas reduces the formation of NO_2, with the addition of reformate gas 1 being more effective;**
- **At $\phi = 0.9$, the addition of reformate gas 2 is more effective to reduces the formation of NO_2 than that of reformate gas 1.**

N_2O Formation

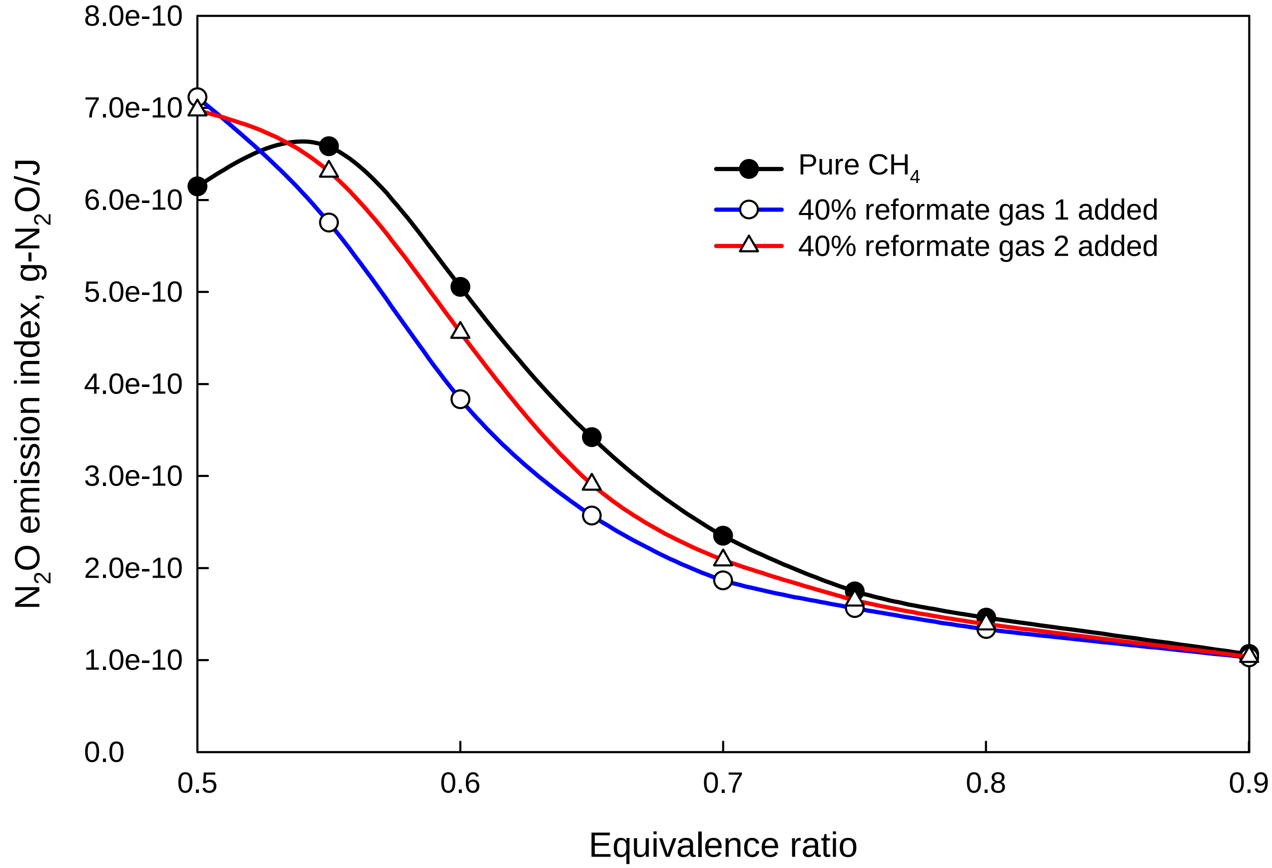

- N_2O (+M) = N_2 + O (+M)
- N_2O + H = N_2 + OH

- **At a constant ϕ, the addition of a reformate gas reduces the formation of N_2O, because of the increase in the N_2O destruction rate;**
- **At a constant enrichment fraction, the formation of N_2O increases with the decrease of equivalence ratio, except for the flame close to extinction.**

Conclusions

- The addition of a reformate gas enlarges the flammable range and lowers the flammability limit of stretched lean CH_4/air premixed flame;
- The reformate gas enrichment allows a combustor to operate at leaner condition;
- Although the addition of a reformate gas may increase the formation of NO at a constant equivalence ratio, it can significantly reduce the emission of NO by allowing a combustor to operate under leaner condition;
- At a leaner operating condition, the formation of NO_2 and N_2O relatively increases. However, the addition of a reformate gas can moderate this effect.

NRC CNRC

Institute for Chemical Process and Environmental Technology

Science at work for Canada

National Research Council Canada

Conseil national de recherches Canada

Canada